# Slow Spin Relaxation in a Low-Spin S=1/2 Fe^{III} Carborane Complex

Ana B. Buades,[a] Victor S. Arderiu,[a] Lindley Maxwell,[b,c] Martín Amoza,[b] Duane Choquesillo-Lazarte,[d] Núria Aliaga-Alcalde,[a,e] Clara Viñas,[a] Francesc Teixidor[a*] and Eliseo Ruiz[b]

IN THIS COMMUNICATION, WE REPORT THE FIRST EVIDENCE OF SLOW-SPIN RELAXATION OF A LOW-SPIN FEIII CARBORANE COMPLEX. IRON S=1/2 COMPLEXES SHOWING SUCH BEHAVIOUR ARE SPECIALLY APPEALING AS QUBITS CANDIDATES BECAUSE THEY FULFIL SOME OF THE MAIN REQUIREMENTS TO REACH LONG DECOHERENCE TIMES: MODERATE MAGNETIC ANISOTROPY, SMALL SPIN, METAL ELEMENT MAINLY WITH ZERO-NUCLEAR SPIN AND FURTHERMORE, LARGE VERSATILITY TO INTRODUCE CHEMICAL MODIFICATIONS.

During the last few years, some research groups have been working in the synthesis of new metal complexes that could be candidates to play a significant role in qubit devices for quantum computers.[i] Up to now, microwave superconductor resonators are good candidates to build up a dense 2D network of qubits in a single device.[ii] Usually, magnetic S=1 nitrogen-vacancy (NV) centres in diamond have been used due to its relative long decoherence T_2 time (around 10 ms) despite their highly complicate synthesis procedure (high energy irradiation during long periods).[iii] Magnetic molecules with small spin values could be an alternative if they can reach high decoherence times, so far, the best ones are S=1/2 V^{IV} complexes presenting time coherence values of 0.01 ms.[iv] The main requirements to improve such values are fulfil by (i) low-spin complexes with small anisotropy (first row transition metals with small spin-orbit contributions instead of heavier transition metals, such as rare-earth complexes), (ii) metal centres with zero nuclear spins (such as V, Cr or Fe), (iii) rigid coordination modes between the metal centre and ligands and, if possible, (iv) ligands with atoms with zero nuclear spin.[v]

Connecting with the above, the study of new complexes formed when main groups, *d*- or *f*-block metals, are incorporated in multicage carborane species has attracted a great interest due to its added value in several applications.[vi] Among this group, the most known metallabis(dicarbollide) systems are the ones whose general formula is [3,3'-M(1,2-C$_2$B$_9$H$_{11}$)$_2$]$^-$, (M = Co, Fe).[vii] These complexes consist of two η^5-carboranyl ligands, *nido*-[7,8-C$_2$B$_9$H$_{11}$]$^{2-}$, and a M^{III} metal located in between. The η^5-carboranyl moiety possesses 6π electrons delocalized in the open pentagonal [C$_2$B$_3$H$_5$]$^{2-}$ face, similar to the metal-bonding orbitals of the cyclopentadienyl ligand [C$_5$H$_5$]$^-$. In fact, ferrocene is neutral, the hydrogen atoms bonded to the carbons beam out of the centre of the aromatic ring. Substituents, which can only be at one plane are largely coplanar with the pentagonal [C$_5$H$_5$]$^-$ ring (see Scheme 1). Conversely, ferra(bisdicarbollide) is monoanionic where the hydrogen atoms beam out of the centre of the icosahedron so, the substituents can therefore be located at different planes and are noncoplanar with the pentagonal [C$_2$B$_3$]$^{2-}$ face.
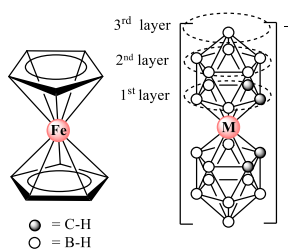

Scheme 1. Schematic representation of neutral ferrocene and the anionic metallabis(dicarbollide) sandwich complexes.

The interest in these metallabis(dicarbollide) sandwich molecules derives from the multiple properties that they possess: they have one negative charge distributed throughout the volume of the complex; are electroactive compounds with a low charge density,[viii] show thermal and chemical stability[via] and an amphiphilic character,[ix] as well. This richness explains the many attempts to suggest new metallabis(dicarbollide) derivatives applicable to materials science[x] as an electroactive species in sensors[xi] and biosensors,[xii] as a doping agent in conducting organic polymers,[vih] as extracting agents of radionuclides from nuclear waste,[xiii] in dye-sensitized solar cells,[xiv] in medicine[xv] and in several other fields.

Now, satisfying most of the criteria described before toward the design of qubit systems, a metallabis(dicarbollide) complex has been magnetically characterized. For that, good quality crystals of [NMe$_4$][3,3'-Fe(1,2-C$_2$B$_9$H$_{11}$)$_2$] were grown as red plates by slow evaporation from a mixture of acetonitrile : water (1:1).[xvi] The crystal structure reveals two orientations of the [NMe$_4$][3,3'-M(1,2-C$_2$B$_9$H$_{11}$)$_2$] molecules, arranged in infinite zig-zag chains (see Figure 1, see ESI for more structural details). Each chain is held together by C$_c$–H···H(7')–B(7') dihydrogen bonds that involve a protonic C$_c$-H atom from one complex and one B-H vertex of the neighbouring one (with a distance and angle of 2.036 Å and 133.5°, respectively). It is important to emphasize that direct interactions between the anionic [3,3'-

Fe(1,2-C$_2$B$_9$H$_{11}$)$_2$]$^-$ complexes are observed in the supramolecular structure while the [NMe$_4$]$^+$ cations surround the supramolecular 1D anionic chain by intermolecular C$_{complex}$–H···H–C$_{NMe4}$ interactions with H···H distances of 2.036Å.
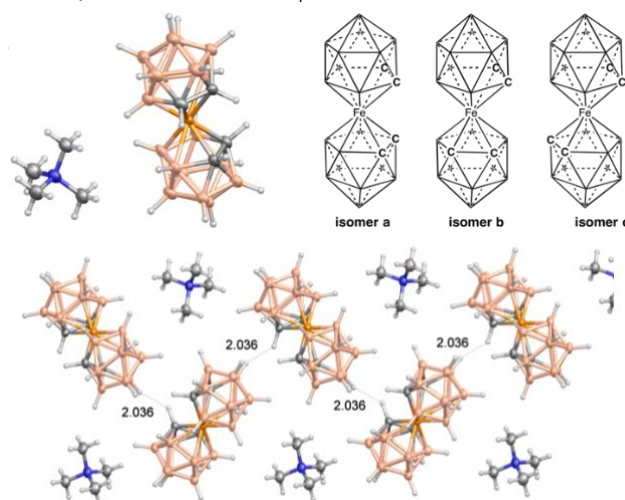
Figure 1. Top left: Molecular representation of [NMe$_4$][3,3'-Fe(1,2-C$_2$B$_9$H$_{11}$)$_2$]; colour legend: C = grey, H = white, N = blue, Fe = yellow and B = pink. Top right: isomers a-c. Bottom: packing displaying a 1D supramolecular chain and the C$_c$-H···B-H intermolecular interactions.

Concerning the magnetic studies, the powder sample of [NMe$_4$][3,3'-Fe(1,2-C$_2$B$_9$H$_{11}$)$_2$] did not show slow spin-relaxation (see Fig. 7) so we pursued solution studies of the complex in THF. SQUID temperature dependence ac measurements were performed using an external field of 0.05 T (no slow-relaxation was found at zero field, see ESI Figs. S6 and S7). In addition, our complex displays the possibility of conversion between isomers (*a-c*, Fig. 1 Top right) by changing the relative position of the C$_2$ units between the two ligands. In this regard, our DFT calculations show that the *a* isomer (present in the X-ray structure) is less stable than the *c* isomer (see Table S3). Furthermore, there was an important change in the calculated *g* components for such isomers (see Table S7). Thus, we also performed EPR measurements in powder and THF solution (see Fig S8) to check if there was a considerable variation in the g values caused by the isomerization when the sample was solved in THF. Figure S8 shows the experimental and simulated EPR experiments revealing that there is an important reduction of the anisotropic character (see fitted *g* components in Fig. S8) when the sample was solved (see a similar change due to the isomerization in the susceptibility and magnetization in Fig. S9). This is consistent with the conversion of the *a* isomer to the more stable ones (confirming, as it was seen with the DFT calculations that *such* isomer is the less stable for isolated molecules or in solution).

Figure 2 shows Cole-Cole diagrams of the system and the fitting of the data using a Debye generalized model (CC-FIT program, see ESI for analytical expressions).[xvii] Spin relaxation times (τ values) were determined at each given temperature (Table S9 and Fig. S7). Using the τ values, the spin relaxation mechanism was studied by analysing the dependence of τ with the temperature by means of the following equation assuming a constant external magnetic field *H*:

$$t^{-1} = AH^4T + \frac{B_2}{1 + B_1H^2} + d\frac{1 + eH^2}{1 + fH^2}T^n$$

(1)
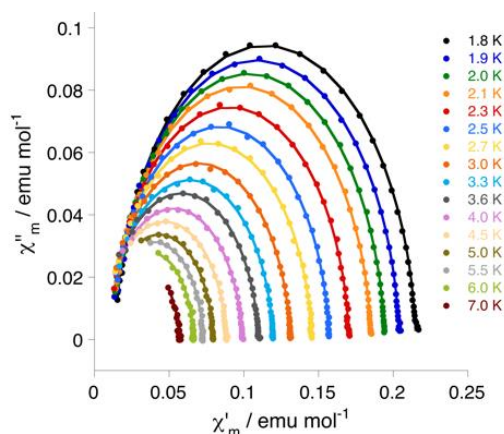
Figure 2. Cole-Cole diagram for a saturated THF solution of [NMe$_4$][3,3'-Fe(1,2-C$_2$B$_9$H$_{11}$)$_2$] under an external field of 0.05 T (see ESI Figure S7).

The terms in Eq. 1 refer to direct relaxation, quantum tunnelling and Raman, respectively, while Orbach phenomena was not considered because of the system under study is S=$^1/_2$. The Raman term corresponds to the field-dependent term using the Brons-van Vleck equation and the typical power law dependence with the temperature.[xviii]
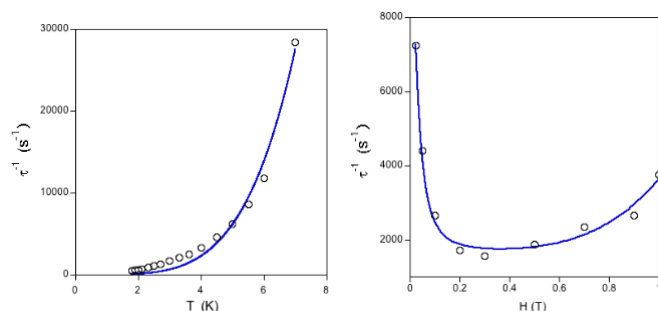
Figure 3. Dependence of the inverse spin-relaxation times, τ^{-1} vs. temperature for a saturated THF solution of [NMe$_4$][3,3'-Fe(1,2-C$_2$B$_9$H$_{11}$)$_2$] under an external field (H) of 0.05 T (left) and with an external field at 4 K (right). The blue lines show the fitted values using Eqs. 2 (left) and 3 (right), respectively.

Figure 3 left (τ^{-1} vs. T) shows a clear relationship with the Raman term. However, the quantum tunnelling term, that in some cases is the responsible of the spin relaxation when using low external fields, appears almost negligible in this case (Fig. 3 right), where both curves shown in Fig. 3 can be analysed using the Raman contribution and including only the direct term at high external fields. Here, the quantum tunnelling mechanism (that depends of the intermolecular magnetic dipolar interactions) does not rule as a consequence of the application of an external field and the use of a solution sample with longer intermolecular distances than powder samples. To avoid overparametrization in the fitting, the Raman term was used exclusively (the direct term was only considered for the field dependence, see later). This way, Eq. 1 was rationalised as:

$$t^{-1} = CT^n \qquad (2)$$

The fitting of the data provided values of C = 4.74 s^{-1}K$^{-4.45}$ and n = 4.45. The Raman term has usually n values between 4 and 9, depending of the vibrational states of the system, being this one in the expected range.[xix] We adjusted the field-dependent data (see Eq. 3) with the field dependent Raman term and with the inclusion of the direct term, which becomes predominant above 0.3 T (see Figure 3 right). The spin relaxation dependence with the external field (see Table S10) using Eq. 3 gave rise to d=11.75 s^{-1} (this value is constrained in the fit to be consistent with the already fitted C value), e=150.9 T^{-2}, f=966.0 T^{-2} and A =490.4 s^{-1}T^{-4}K^{-1} values. The AH^4T direct term at H = 0.05 T is negligible justifying the fact that we disregarded such value in Eq. 2.

The magnetic anisotropy of [3,3'-Fe(1,2-C$_2$B$_9$H$_{11}$)$_2$]$^-$ complex was corroborated by *ab initio* NEVPT2 calculations,[xx] including spin-orbit effects (Quasi Degenerate Perturbation Theory)[xxi] using the Orca 4.0 code[xxii] and a def2-TZVPP basis set[xxiii] (three active spaces were tested, see ESI for Computational details). In Figure S6, the static magnetic properties calculated from the *ab initio* calculations were compared with the experimental ones with reasonable agreement. The calculated components of the diagonal *g* tensor were 1.35, 1.36 and 4.79 (X-ray structure), indicating an axial magnetic anisotropy. The analysis of the nature of the ground and first excited states revealed a transition between d$_{xy}$ and d$_{x^2-y^2}$ orbitals (Fig. 4 *ab initio* Ligand Field Theory orbitals (AILFT) and Tables S5 and S8 for the orbital energies).[xxiv]

$$t^{-1} = d\frac{1+eH^2}{1+fH^2}4^{4.45} + A\cdot4\cdot H^4 \qquad (3)$$

To understand the relatively large magnetic axial anisotropy found for the [3,3'-Fe(1,2-C$_2$B$_9$H$_{11}$)$_2$]$^-$ complex, we analysed the orbital splitting. Remarkably, the analysis of the ground state wave function revealed that the orbital occupancy was determined by the different electronic repulsion of the orbitals instead of their energy (Fig. 4). Thus, the d$_{z^2}$ orbital remains doubly occupied while ground and first excited states correspond to the alternation of single and double occupations of the d$_{x^2-y^2}$ and d$_{xy}$ orbitals, in that order. This anomalous orbital occupancy for d^5 metallocene systems has already been reported and spectroscopic data of these complexes have shown consistency with a high field configuration.[xxv]
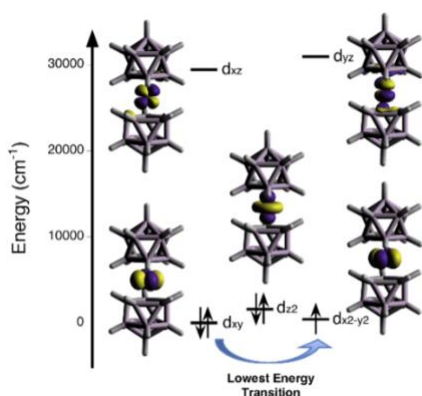
Figure 4. Orbital splitting of the [3,3'-Fe(1,2-$C_2B_9H_{11}$)$_2$]$^-$ complex obtained with the AILFT method using the NEVPT2 wave function.

In this context, the g components can be expressed as functions of the orbital energies and integrals:

$$g_{kl} = g_e + \frac{\zeta_{eff}}{2S} \sum_{i,p} \frac{\langle \varphi_i | l_k | \varphi_p \rangle \langle \varphi_p | l_l | \varphi_i \rangle}{\varepsilon_p - \varepsilon_i} - \frac{\zeta_{eff}}{2S} \sum_{p,a} \frac{\langle \varphi_p | l_k | \varphi_a \rangle \langle \varphi_a | l_l | \varphi_p \rangle}{\varepsilon_a - \varepsilon_p}$$

(4)

where ζ_{eff} is the spin-orbital coupling constant, l_k is the k-component of the angular momentum operator and φ are the molecular orbitals (with orbital energy ε) with the subindex i, p or a to indicate double-occupied, singly-occupied or empty orbitals, respectively. Here, the orbital occupancy found for the [3,3'-Fe(1,2-$C_2B_9H_{11}$)$_2$]$^-$ complex show quasi degeneracy between the $d_{x^2-y^2}$ and d_{xy} orbitals, involved in the first excitation. The loss of magnetic anisotropy due to the isomerization of the X-ray structure in solution (Tables S6 and S7) is directly related to the high difference between such two orbitals in the most stable isomers (Tables S5 and S8). In addition, the integrals (Eq. 4) involving the l_z component of the angular momentum for these two orbitals are different than zero (they have the same $|m_l|$ value). The synergy of the two factors generates the large g_z value (calculated, Tables S6 and S7) and consequently, they are the origin of the magnetic anisotropy experimentally found.

Conclusions

A S=$^1/_2$ carborane compound, [NMe$_4$][3,3'-Fe(1,2-$C_2B_9H_{11}$)$_2$], has been structurally and magnetically characterised. Despite of the small spin, the system presents slow relaxation of the magnetization and such behaviour can be corroborated with *ab initio* NEVPT2 calculations showing a relatively large magnetic anisotropy. The origin of such anisotropy relates to the near degeneracy pictured for the low-spin d^5 electron configuration having the first excitation between $d_{x^2-y^2}$ and d_{xy} which in addition have the same $|m_l|$ value, leading to a large axial contribution of the magnetic anisotropy.

Acknowledgements

Conflicts of interest

There are no conflicts to declare

---

i (a) J. M. Zadrozny, J. Niklas, O. G. Poluektov and D. E. Freedman, *ACS Cent. Sci.*, 2015, **1**, 488. (b) 1 G. Aromí, D. Aguilà, P. Gamez, F. Luis and O. Roubeau, *Chem. Soc. Rev.*, 2012, **41**, 537. (c) E. Moreno-Pineda, C. Godfrin, F. Balestro, W. Wernsdorfer and M. Ruben, *Chem. Soc. Rev.*, 2017, **47**, 501.

ii Bonizzoni, A. Ghirri, K. Bader, J. van Slageren, M. Perfetti, L. Sorace, Y. Lan, O. Fuhr, M. Ruben and M. Affronte, *Dalt. Trans.*, 2016, **45**, 16596.

iii (a) B. B. Buckley, G. D. Fuchs, L. C. Bassett and D. D. Awschalom, *Science*, 2010, **330**, 1212. (b) B. J. Maertz, A. P. Wijnheijmer, G. D. Fuchs, M. E. Nowakowski and D. D. Awschalom, *Appl. Phys. Lett.*, 2010, **96**, 92504.

iv M. Atzori, E. Morra, L. Tesi, A. Albino, M. Chiesa, L. Sorace and R. Sessoli, *J. Am. Chem. Soc.*, 2016, **138**, 11234.

v (a) M. S. Fataftah, J. M. Zadrozny, S. C. Coste, M. J. Graham, D. M. Rogers and D. E. Freedman, *J. Am. Chem. Soc.*, 2016, **138**, 1344. (b) 1 J. M. Zadrozny and D. E. Freedman, *Inorg. Chem.*, 2015, **54**, 12027. (c) M. Atzori, L. Tesi, S. Benci, A. Lunghi, R. Righini, A. Taschin, R. Torre, L. Sorace and R. Sessoli, *J. Am. Chem. Soc.*, 2017, **139**, 4338. (d) M. Atzori, L. Tesi, E. Morra, M. Chiesa, L. Sorace and R. Sessoli, *J. Am. Chem. Soc.*, 2016, **138**, 2154.

vi (a) J. Plesek, *Chem. Rev.,* 1992, **92**, 269; (b) R.N. Grimes in *Carboranes*, Carboranes, 3rd Ed., Elsevier Inc. 2016; (c) S. V. Timofeev, I. B. Sivaev, E. A. Prikaznova and V. I. Bregadze, *J. Organomet. Chem.*, 2014, **751**, 221; (d) N. P. E. Barry and P. J. Sadler, *Chem. Soc. Rev.*, 2012, **41(8)**, 3264; (e) L. Deng and Z. W. Xie, *Coord. Chem. Rev.*, 2007, **251**, 2452; (f) R. Núñez. I. Romero, F. Teixidor and C. Viñas, *Chem. Soc. Rev.*, 2016, **45**, 5147; (g) N. S. Hosmane and J. A. Maguire, Comprehensive Organometallic Chemistry III, 3th Ed., 2007, 175-264; (k) H. W. Roesky, S. Singh, K .K. M. Yusuff, J. A. Maguire and N. S. Hosmane, *Chem. Rev.,* 2006, *106,* 3813.

vii M. F. Hawthorne and T. D. Andrews, *Chem. Commun.*, 1965, **19**, 443.

viii C. Masalles, J. Llop, C. Viñas and F. Teixidor, *Adv. Mater.,* 2002, **14(11)**, 826.

ix (a) R.N. Grimes, Advanced Inorganic Chemistry, 6th Ed., (Eds: F. A. Cotton, G. Wilkinson, C. A. Murillo, M. Bochmann), 1999, 143; (b) P. Bauduin, S. Prevost, P. Farras, F. Teixidor, O. Diat and T. Zemb, *Angew. Chem. Int. Ed.,* 2011, **50**, 5298; (c) M. Uchman, V. Dordovi, Z. Tosner and M. Pavel, *Angew. Chem. Int. Ed.* 2015, **54**, 14113.

x (a) M. F. Hawthorne, J. I. Zink, J. M. Skelton, M. J. Bayer, C. Liu, E. Livshits, R. Baer and D. Neuhauser, *Am. Assoc. Adv. Sci. Pub.*, 2004, **303**, 1849; (b) A. K. Singh, A. Sadrzadeh and B. I. Yakobson, *J. Amer. Chem. Soc.*, 2010, **132**, 14126; (c) J. Zhang and Z. Xie, *Acc. Chem. Res.*, 2014, **47**, 1623; (d) S. M. Gao and N. S. Hosmane, *Russ. Chem. Bull.* 2014, **63**, 788; (e) C. Viñas, F. Teixidor and R. Nuñez, *Inorg. Chim. Acta*, 2014, **409**, 12.

xi (a) A. I. Stoica, C. Viñas and F. Teixidor, *Chem. Commun.*, 2008, 6492; (b) A. I. Stoica, C. Viñas and F. Teixidor, *Chem. Commun.,* 2009, 4988.

xii (a) T. Garcia-Mendiola, V. Bayon-Pizarro, A. Zaulet, I. Fuentes, F. Pariente, F. Teixidor, C. Viñas and E. Lorenzo, *Chem. Sci.,* 2016, **7**, 5786; (b) I. Grabowska, A. Stachyra, A. Gora-Sochacka, A. Sirko, A. B. Olejniczak, Z. J. Lesnikowski, J. Radecki and H. Radecka, *Biosens Bioelectron.*, 2014, **51**, 170; (c) R. Ziolkowski, A. B. Olejniczak, L. Gorski, J. Janusik, Z. J. Lesnikowski and E. Malinowska, *Bioelectrochemistry*, 2012, **87**, 78.

xiii (a) C. Viñas, S. Gómez, J. Bertrán, F. Teixidor, J. Dozol and H. Rouquette, *Chem. Commun.*, 1998, 191; (b) C. Viñas, S. Gómez, J. Bertrán, F. Teixidor, J. Dozol and H. Rouquette, *Inorg. Chem.,* 1998, **37**, 3640; (c) B. Grüner, J. Plesek, J. Báca, I. Cisarová, J. Dozol, H. Rouquette, C. Viñas, P. Selucký and J. Rais, *New J. Chem.*, 2002, **26**, 1519; (d) M. Bubenikova, P. Selucky, J. Rais, B. Gruner and P. Svec, *J. Radioanal. Nucl. Chem.*, 2012, **293**, 403; (e) B. Gruner, P. Svec, Z. Hajkova, I. Cisarova, J. Pokorna and J. Konvalinka, *Pure Appl. Chem.*, 2012, **84**, 2243.

xiv T. C. Li, A. M. Spokoyny, C. She, O. K. Farha, C. A. Mirkin, T. J. Marks and J. T. Hupp, *J. Am. Chem. Soc.*, 2010, **132**, 4580.

xv (a) Z. Lesnikowski, *J. Med. Chem.*, 2016, **59**, 7738; (b) M. Scholz and E. Hey-Hawkins, *Chem. Rev.*, 2011, **111**, 7035; (c) P. Cígler, M. Kožíšek, P. Řezáčová, J. Brynda, Z. Otwinowski, J. Pokorná, J. Plešek, B. Grüner, L. Dolečková-Marešová, M. Máša, J. Sedláček, J. Bodem, H. G. Kräusslich, V. Král and J. Konvalinka, *Proc. Natl. Acad. Sci. U.S.A.*, 2005, 102(43), 15394; (e) J. F. Valliant, K. J. Guenther, A. S. King, P. Morel, P. Schaffer, O. O. Sogbein and K. A. Stephenson, *Coord. Chem. Rev.*, 2002, **232**, 173.

xvi **Crystal Data.** $C_8H_{34}B_{18}NFe$, M_r = 394.79, Monoclinic, Cc, a = 6.8764(3) Å, b = 28.8263(5) Å, c = 10.7581(5)Å, β = 91.2940(10) °, V = 2131.94(18) Å3, T = 100 K, Z = 4, λ = 0.82654 Å, μ = 1.056, 12144 reflections measured, 3506 unique (R_{int} = 0.0925) which were used in all calculations. The final wR_2 was 0.1472 (all data) and R_1 was 0.0610 (I≥σ(I)). CCDC 1585386

xvii Y.-N. Guo, G.-F. Xu, Y. Guo and J. Tang, *Dalt. Trans.*, 2011, **40**, 9953.

xviii J.H. Van Vleck, *Phys. Rev.*, 1940, **57**, 426.

xix K. N. Shrivastava, *Phys. Status Solidi*, 1983, **117**, 437.

xx C. Angeli, R. Cimiraglia, S. Evangelisti, T. Leininger and J.-P. Malrieu, *J. Chem. Phys.* 2001, **114**, 10252; C. Angeli, R. Cimiraglia and J.-P. Malrieu, *Chem. Phys. Lett.* 2001, **350**, 297; C. Angeli, R. Cimiraglia and J.-P. Malrieu, *J. Chem. Phys.* 2002, **117**, 9138.

xxi H. Nakano, R. Uchiyama and K. Hirao, *J. Comput. Chem.*, 2002, **23**, 1166.

xxii F. Neese, *Wiley Interdiscip. Rev. Comput. Mol. Sci.*, 2018, **8**, e1327.

xxiii (a) F. Weigend and R. Ahlrichs, *Phys. Chem. Chem. Phys.* 2005, **7**, 3297; (b) A. Schaefer, H. Horn and R.J. Ahlrichs, *J. Chem. Phys.* 1992, **97**, 2571.

xxiv F. Weigend and R. Ahlrichs, *Phys. Chem. Chem. Phys.* 2005, **7**, 3297; A. Schaefer, H. Horn and R.J. Ahlrichs, *J. Chem. Phys.* 1992, **97**, 2571.

xxv K.D. Warren, *Structure and Bonding*, 1976, **27**, 45.